Appl Phys A (2009) 97: 157–165
DOI 10.1007/s00339-009-5284-1

**Applied Physics A**
**Materials Science & Processing**

# Effect of nickel nanofillers on the dielectric and magnetic properties of composites based on rubber in the X-band

**E. Muhammad Abdul Jamal · P. Mohanan · P.A. Joy · Philip Kurian · M.R. Anantharaman**

Received: 2 February 2009 / Accepted: 13 May 2009 / Published online: 29 May 2009


**Abstract** Nickel–rubber nanocomposites were synthesized by incorporating ferromagnetic nickel nanoparticles in a natural rubber as well as neoprene rubber matrix. Complex dielectric permittivity and magnetic permeability of these composites were evaluated in the X-band microwave frequencies at room temperature using cavity perturbation technique. The dielectric loss in natural rubber is smaller compared to neoprene rubber. A steady increase in the dielectric permittivity is observed with increase in the content of nickel in both the composites. The magnetic permeability exhibits a steady decrease with increase in frequency and magnetic loss shows a relaxation at 8 GHz. The suitability of these composites as microwave absorbers is modeled based on the reflection loss which is dependant on the real and imaginary components of the complex dielectric permittivity and magnetic permeability.

**PACS** 75.75.+a · 77.22.Gm · 75.50.-y

E.M.A. Jamal · M.R. Anantharaman (✉)
Department of Physics, Cochin University of Science and Technology, Cochin 22, Kerala, India
e-mail: mraiyer@yahoo.com
Fax: +91-484-2577595

E.M.A. Jamal
e-mail: emajamal@yahoo.co.in
Fax: +91-484-2577595

P. Mohanan
Department of Electronics, Cochin University of Science and Technology, Cochin 22, India
e-mail: drmohan@cusat.ac.in
Fax: +91-484-2577595

P.A. Joy
National Chemical Laboratory, Pune, India
e-mail: pa.joy@ncl.res.in
Fax: +91-(0)20-25902601

P. Kurian
Department of Polymer Science and Rubber Technology, Cochin University of Science and Technology, Cochin 22, India
e-mail: pkurian@cusat.ac.in

## 1 Introduction

The interest in electromagnetic absorbers in the microwave region has increased in recent times due to the significant expansion in applications using electromagnetic waves in this frequency band. There are numerous electronic gadgets operating in the microwave frequencies like mobile phones, wireless local area networks, and radar systems, and the problem of electromagnetic interference has worsened significantly necessitating the use of microwave absorbers [1, 2]. A good absorber has to have low or negligible reflection, sufficiently large attenuation, and good heat dissipation characteristics because the absorbed energy is converted to heat within the material [3]. In stealth technology, which is another important field of application of microwave absorption, total absorption of electromagnetic waves without any reflection is essential since the device should go undetected by radar signals.

The complex dielectric permittivity and magnetic permeability of a material together defines its electromagnetic wave absorbing characteristics and this emphasizes the importance of magnetic dielectric materials. Various kinds of magnetic dielectric materials have been developed over the years to find application as microwave absorbers, such as ferrites, ferrite–polymer composites, and composites containing metallic magnetic particulates [4–9]. In comparison to ferrites, metallic magnetic composites have several advantages like high saturation magnetization, tunability of

magnetic permeability by controlling the volume fraction of metallic particles, mechanical flexibility of the host material of the composite. One major disadvantage of metallic magnetic composite is the drop in magnetic permeability at higher applied frequencies due to skin effect and eddy current loss developed in the particulates [10]. However, this drawback can be overcome by using particles of size smaller than the skin-depth of the metal with respect to the frequency of operation. The skin depth of iron in gigahertz frequencies has been estimated to be about 1 μm and that of nickel 500 nm [11]. Iron and nickel particles below these critical size limits dispersed in suitable dielectric materials therefore are potential candidates as microwave absorbers.

In this article we describe the investigations on the complex dielectric and magnetic properties of composites prepared by impregnating nanometer-sized nickel particles in two different elastomer matrixes namely natural rubber and neoprene rubber. Natural rubber is an easily available and inexpensive material and neoprene is a synthetic rubber with several superior physical properties compared to natural rubber, such as better resistance to harsh chemicals, to flame, and to salinity [12]. The ease in moulding into any shape and size can give both of these materials an extra edge in stealth applications. The complex dielectric permittivity and magnetic permeability of these composites are evaluated in the X-band microwave frequency from 7 to 12 GHz and based on this the input impedance and the reflection loss are calculated. The suitability of the composites as the potential microwave absorbers is also examined.

## 2 Experimental details

### 2.1 Synthesis and characterization of nickel nanoparticles

Nickel particles were synthesized by the authors using a modified sol–gel combustion process (patent pending—atent application No. 1927/07/Indian patent). Better particle size reduction was achieved by employing this modified process. To further reduce the size of the particles below 100 nm the synthesized powder was subjected to high-energy ball milling using a Fritsch planetary ball mill model P-7 for around 2 h. The structural studies of nickel particles were carried out by means of X-ray diffractometry (XRD) (Rigaku Dmax C with Cu K$\alpha$ X-ray source of wavelength of 1.54 Å). Superconducting quantum interference device magnetometry (SQUID) was employed for evaluating the magnetic properties (MPMS-5S XL Quantum Design magnetomer).

### 2.2 Preparation of rubber–nickel nanocomposites

Precharacterized nickel particles were used for the preparation of the composites by incorporating nickel powder into natural rubber as well as in neoprene rubber according to specific recipes reported elsewhere [13, 14]. Six sets of composites were prepared with content of nickel particles ranging from 0 to 100 phr (parts per hundred rubber) in steps of 20 phr. The compounds were compression-moulded into sheets of about 2-mm thick using an electrically heated hydraulic press having 45 cm × 45 cm platens at a pressure of 140 kg/cm$^2$ in a standard mould and cured up to their respective cure times at their curing temperatures. (150°C for natural rubber and 160°C for neoprene rubber.) The magnetic hysteresis loop parameters of the composites were evaluated by using an EG&G PAR 2000 vibrating sample magnetometer.

### 2.3 Evaluation of complex dielectric permittivity and magnetic permeability

Rectangular strips of about 5 cm in length and 2 mm × 2 mm in cross section were cut from the sheets of composites and the dielectric measurements in the X-band microwave frequencies were done by cavity perturbation method using an Agilent 4-port network analyzer with a rectangular cavity of dimensions 1 cm × 2.3 cm × 15.1 cm. The cavity has a precision cut hole at the center (along the 2.3-cm side) through which the sample can be introduced and dielectric measurements were carried out at odd modes (electric field forms an antinode at the center) and permeability measurements at even modes (electric field forms a node at the center) [15, 16]. The equations used for determining the complex permittivity and permeability are given in the following section.

For a rectangular cavity, real part of the dielectric permittivity ($\varepsilon'_r$) can be calculated from the relation [16]

$$\frac{\Delta f}{f_s} = 2\frac{V_s}{V_c}(\varepsilon'_r - 1) \tag{1}$$

where $\Delta f$ is the shift in resonance frequency on introduction of the sample into the cavity and $V_s$ and $V_c$ are the volumes of the sample and the cavity, respectively.

The imaginary part of the dielectric permittivity ($\varepsilon''_r$) can be calculated using the equation

$$\left[\frac{1}{2Q_s} - \frac{1}{2Q_c}\right] = 2\frac{V_s}{V_c}\varepsilon''_r \tag{2}$$

$Q_s$ and $Q_c$ are the quality factors of the cavity with and without sample, given by

$$Q_s = \frac{f_s}{\Delta f}, \qquad Q_c = \frac{f_c}{\Delta f} \tag{3}$$

Magnetic permeability was measured by perturbing the cavity by the samples at positions where the electric field is zero. X-band measurements were possible only for even

modes since this cavity was provided with a hole at the center of the cavity. The real and imaginary parts of the complex permeability ($\mu'_r$ and $\mu''_r$) of composite samples were determined using the relations

$$\mu'_r - 1 = \frac{(\lambda_g^2 + 4a^2)}{8a^2}\left(\frac{\Delta f}{f_s}\right)\frac{V_c}{V_s} \tag{4}$$

$$\mu''_r = \frac{(\lambda_g^2 + 4a^2)}{16a^2}\left(\frac{1}{Q_s} - \frac{1}{Q_c}\right)\frac{V_c}{V_s} \tag{5}$$

and

$$\lambda_g = \frac{2l}{p} \tag{6}$$

where $p$ is the number of mode in which the cavity is excited for a particular measurement.

The complex dielectric permittivity values were determined for four different frequencies in the X band. These four frequencies are at nearly 7.224, 8.239, 9.559, and 11.067 GHz corresponding to the $TE_{103}$ to $TE_{109}$ modes of the cavity used for the measurements. The magnetic permeability was measured at five frequencies which are at nearly 6.8746, 7.676, 8.8621, 10.283, and 11.861 GHz corresponding to the $TE_{102}$ to $TE_{1010}$ modes of the cavity.

## 3 Results and discussion

### 3.1 Properties of nickel nanoparticles

The XRD pattern was compared with the published results available in JCPDS files and it was found that the obtained pattern matches exactly with the reported result (JCPDS file no 03-1051). The diffraction peaks were identified and indexed. Particle size D was determined using Debye–Scherrer formula given as

$$D = \frac{0.9\lambda}{\beta \cos\theta} \tag{7}$$

where $\lambda$ is the wavelength of the X-ray source, $\beta$ is the full width at half maximum of the diffraction peaks in radians, and $2\theta$ is the diffraction angle [17]. The average particle size was evaluated and found to be 26 nm. The X-ray diffraction pattern of nickel particles is shown in Fig. 1. The magnetic hysteresis of nickel particles is presented in Fig. 2. The result indicates that the particles are ferromagnetic with coercivity of 68 Oe and remnant magnetization of 8.5 emu/g. The saturation magnetization is found to be 47.5 emu/g and this also is about 87% of the magnetization of a bulk nickel sample which was reported elsewhere [18]. The drop in saturation magnetization is attributed to the formation of dead layer on the surface of nanoparticles [19].

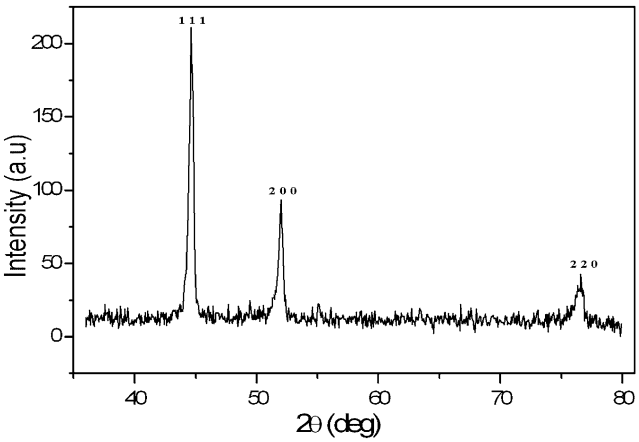


**Fig. 1** XRD of nickel particles

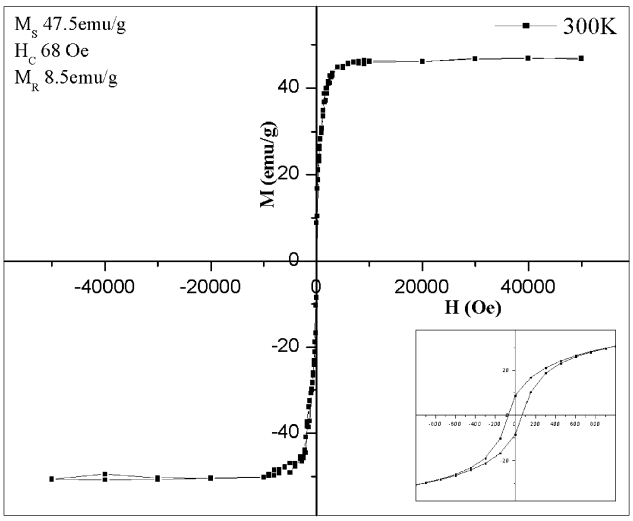


**Fig. 2** Magnetic hysteresis of nickel particles

### 3.2 Magnetic properties of composites

The magnetic hysteresis behavior of the natural-rubber–nickel composites are depicted in Fig. 3 and that of neoprene-rubber–nickel composites are in Fig. 4. All rubber–nickel samples were found to be ferromagnetic in nature. The as-prepared nickel nanoparticles have a saturation magnetization of 47.5 emu/g and the magnetization of the composites were calculated taking the amount of nickel in the composites into account and by assuming that all other components in the composites are nonmagnetic. The saturation magnetization of the composite were calculated by using the equation

$$M_s(composite) = \frac{M_s(nickel) \times m_2}{m_1} \tag{8}$$

where $M_s(composite)$ is the saturation magnetization of the composite, $M_s(nickel)$ is that of nickel particles, $m_1$ is the

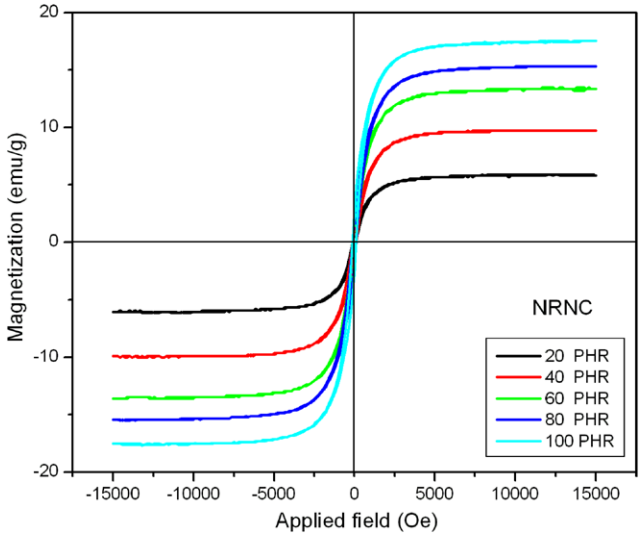


**Fig. 3** Magnetic hysteresis of natural-rubber–nickel composites from 20 to 100 phr

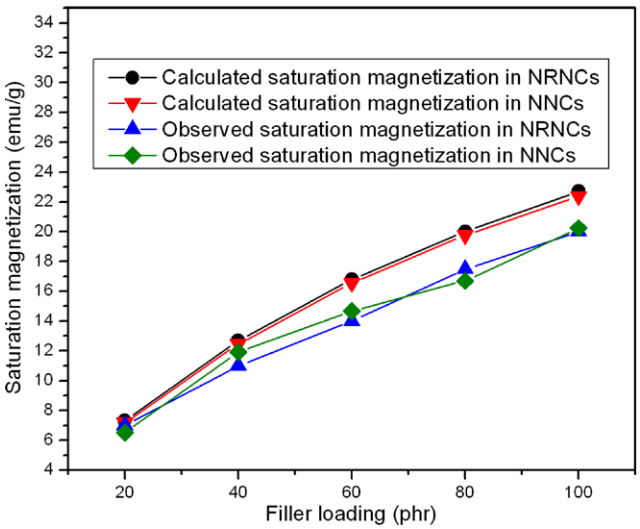


**Fig. 5** Observed and calculated magnetization of natural-rubber–nickel (NRNC) and neoprene-nickel (NNC) composites

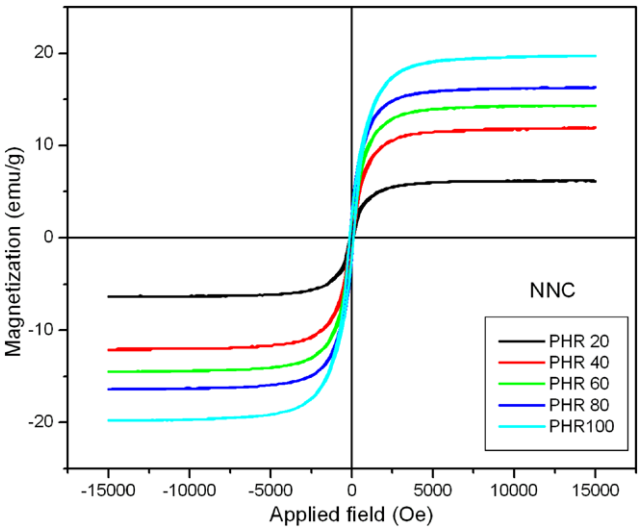


**Fig. 4** Magnetic hysteresis of neoprene-rubber–nickel composites from 20 to 100 phr

mass of a given sample of composite, and $m_2$ is the mass of nickel particles in this sample and they were found to be in good agreement as shown in Fig. 5.

### 3.3 Complex dielectric permittivity of the composites

The variation of the real part of the relative dielectric permittivity ($\varepsilon_r'$) of natural-rubber–nickel composites is depicted in Fig. 6 and that of neoprene-rubber–nickel composites in Fig. 7. It can be observed that, in both types of composites, the permittivity of a particular composite sample remains constant for the entire frequency range of 7–12 GHz. Frequency dependant dispersion of permittivity is completely absent in the X-band frequency. The polarization mechanism operating in the gigahertz frequency is purely electronic or orientational with relaxation times smaller than the time period of the applied signals. Interfacial polarization, which is the basic reason for the dispersion at radio frequency (RF) regime, has no role to play in microwave frequencies as it does not produce dispersion in $\varepsilon_r'$ because of its much smaller relaxation time. But $\varepsilon_r'$ was found to increase with the increase of phr of filler in the composite as it is evident from Figs. 6 and 7. This phenomenon of increase in $\varepsilon_r'$ with the increase in filler concentration can be attributed to the enhancement of electrical conductivity of the composites due to the incorporation of metal particles as filler.

It can be observed from Figs. 6 and 7 that the dielectric permittivity of neoprene-rubber composites are much higher than that of natural-rubber composites for a given filler concentration. Neoprene rubber is made of polar molecules and the polar nature of the molecules is retained even after the cross-linking of the molecule chains. Polar molecules of neoprene can undergo orientational polarization and can give rise to the enhanced polarization compared to the molecules of natural rubber and this explains its higher dielectric permittivity.

Figures 8 and 9 depict the variation in dielectric loss ($\varepsilon_r''$) with frequency of natural-rubber–nickel and neoprene-rubber–nickel composites, respectively. In neoprene-rubber–nickel composites, as frequency increases $\varepsilon_r''$ registers a steady increase and this phenomenon is observed in all the five samples. Even though the absence of interfacial polarization was confirmed from the absence of frequency dispersion of $\varepsilon_r'$, small amount of charge accumulation may be present around metal particles even at gigahertz frequencies. The electric conductance loss may also be contributing at higher frequencies and this could be the reason for enhanced

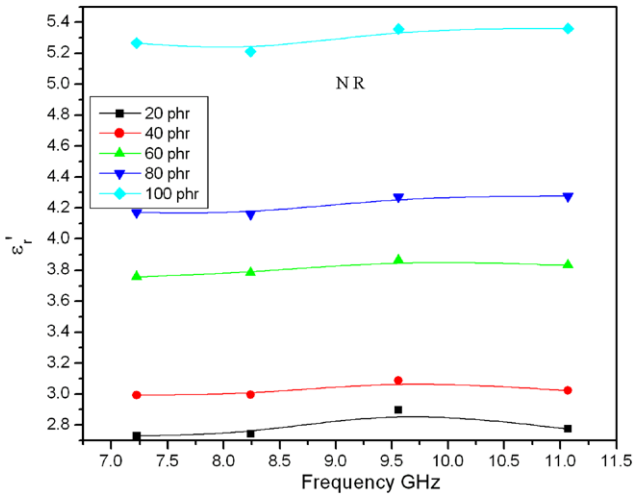


**Fig. 6** Dielectric permittivity of natural-rubber–nickel composites with frequency at different loadings

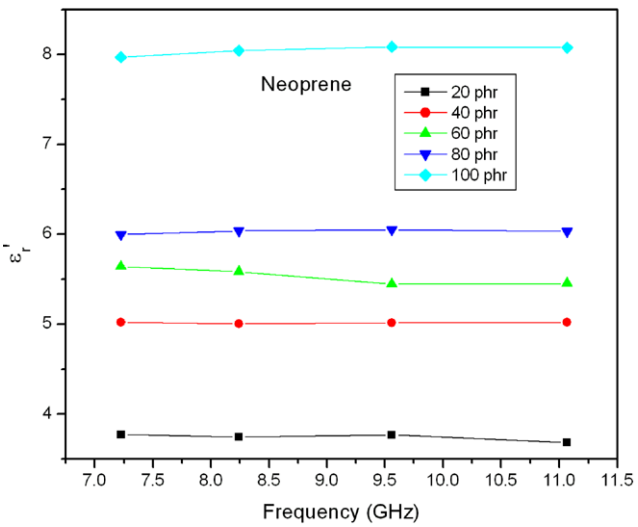


**Fig. 7** Dielectric permittivity of neoprene-rubber–nickel composites with frequency at different loadings

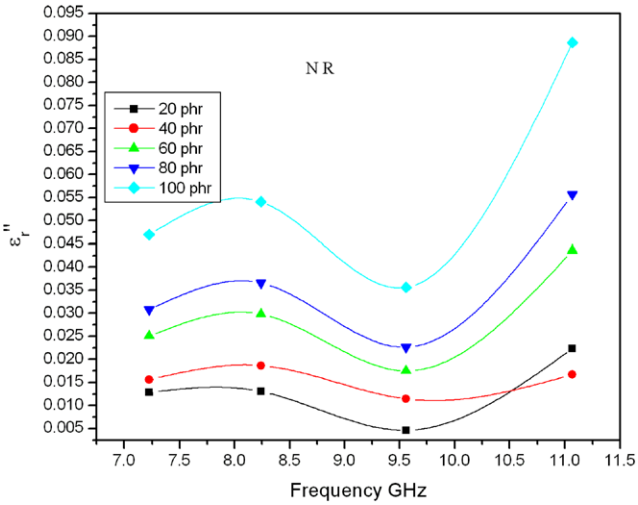


**Fig. 8** Dielectric loss of natural-rubber–nickel composites at different loadings

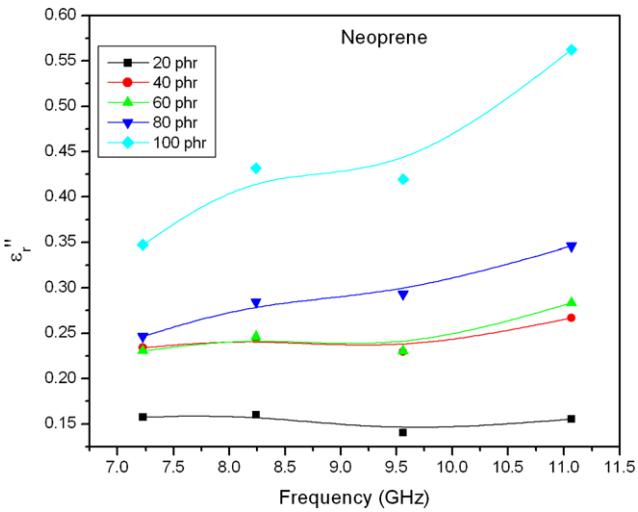


**Fig. 9** Dielectric loss of neoprene-rubber–nickel composites

loss for 100-phr sample towards the higher edge of the frequency band [20]. Also, there is a steady increase in $\varepsilon_r''$ with the increase in the concentration of nickel in the composites suggesting the presence of electrical conductance loss.

Natural-rubber–nickel composites show a similar kind of variation in dielectric loss but at 8.25 GHz there appears a relaxation peak. Orientational polarization of the polymer chains of natural rubber may have a relaxation time close to this frequency causing the relaxation peak. But the dielectric loss increase towards the higher frequency side and increases sharply at higher loading fractions. Conductance loss due to the presence of metallic inclusions is attributed to this enhancement in dielectric loss.

### 3.4 Complex magnetic permeability

The complex permeability studies of the composites reveal that the permeability behavior of both the type of composites is very closely similar. The origin of magnetic permeability is from the embedded ferromagnetic nickel nanoparticles in the matrix and the elastomer matrix does not offer any contribution towards the magnetic properties.

The real part of complex permeability ($\mu_r'$) decreases with the increase in frequency. It is well known that the permeability of ferromagnetic nickel drops sharply in gigahertz frequencies and becomes close to unity at 10 GHz [10]. The influence of skin effect and eddy current loss are present in nanometer-sized particles also, in a reduced magnitude. However, the decrease in $\mu_r'$ is not as sharp as the reported behavior of bulk nickel and this can be attributed

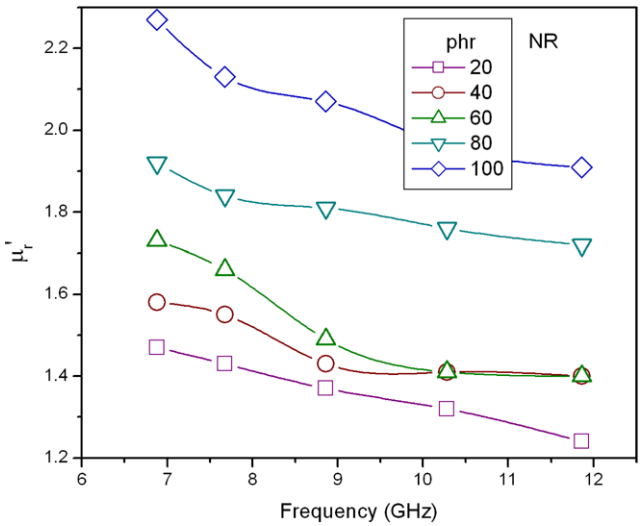


**Fig. 10** Variation of real part of magnetic permeability with frequency for various loadings in natural-rubber–nickel composites

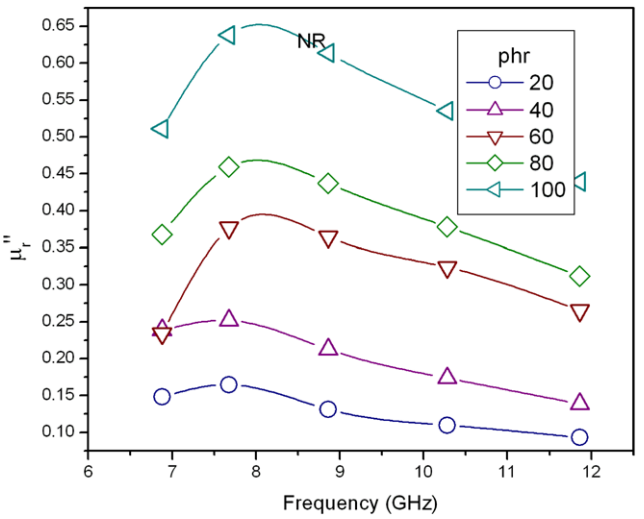


**Fig. 12** Variation of magnetic loss of natural-rubber–nickel composites with frequency for different filler loadings

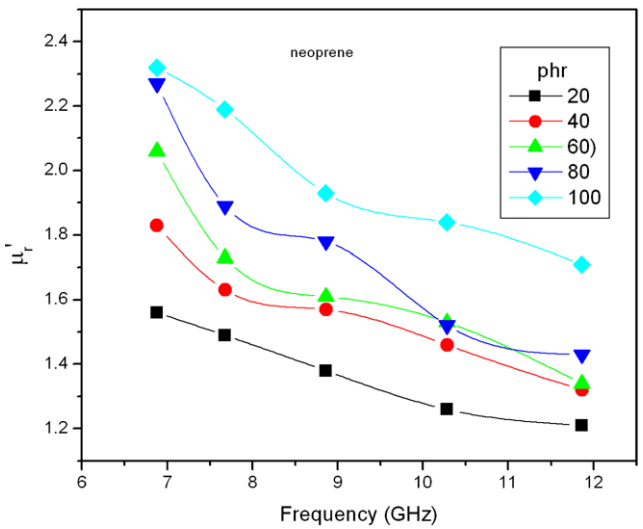


**Fig. 11** Variation of real part of magnetic permeability with frequency for various loadings in neoprene-rubber–nickel composites

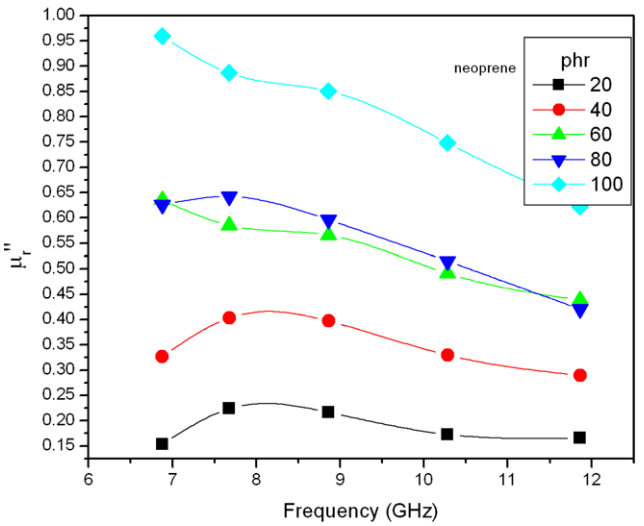


**Fig. 13** Variation of magnetic loss of neoprene-rubber–nickel composites with frequency for different filler loadings

to the reduced size of nickel particle. The variations of $\mu_r'$ with the frequency are shown in Fig. 10 (natural-rubber–nickel composites) and in Fig. 11 (neoprene-rubber–nickel composites).

The magnetic loss ($\mu_r''$) increases initially and both composites show a peak at about 8 GHz and then drops slightly (Figs. 12 and 13). This is attributed to the resonant vibration of the nickel particles in the oscillatory magnetic field [20]. Furthermore, the loss is more pronounced in neoprene-based composites even though the pattern of variation remains the same, as evident from the graphs. It appears that the neoprene matrix offers less resistance to resonant vibrations of nickel particles on application of an oscillatory electromagnetic field.

### 3.5 Input impedance and reflection loss

The microwave absorption characteristics of a material are analyzed on the basis of its complex permittivity and permeability. Good absorbers should have low reflection coefficient and good absorption coefficient. Electromagnetic waves entering a material are absorbed effectively if there is good impedance matching between the material and the free space and the condition for which can be deduced as [21]

$$\frac{\mu'}{\varepsilon'} = 1 \tag{9}$$

The neoprene-nickel composites in our studies shows $\varepsilon_r'$ varying between 2.5 and 5 with respect to different loadings

and $\varepsilon_r'$ varies between 1.2 and 2.2, and it is difficult to meet the condition given by (6) for any particular sample or in any given frequency. The propagation constant $\gamma$ of electromagnetic waves in a material is given by the relation

$$\gamma = \alpha + i\beta \tag{10}$$

here $\alpha$ is the attenuation constant and $\beta$ is the phase constant. In terms of the complex permittivity and permeability the propagation constant is expressed by the relation

$$\gamma = j\frac{2\pi.f}{c}\sqrt{\mu_r\varepsilon_r} \tag{11}$$

Separating the real and imaginary parts of (11) gives the attenuation constant $\alpha$ and the phase constant $\beta$ [21] as

$$\alpha = \frac{\sqrt{2}}{c}\pi.f \times \sqrt{(\mu_r''\varepsilon_r'' - \mu_r'\varepsilon_r') + \sqrt{(\mu_r''\varepsilon_r'' - \mu_r'\varepsilon_r')^2 + (\varepsilon_r'\mu_r'' + \varepsilon_r''\mu_r')}} \tag{12}$$

and

$$\beta = \frac{\sqrt{2}}{c}\pi.f \times \sqrt{(\mu_r'\varepsilon_r' - \mu_r''\varepsilon_r'') + \sqrt{(\mu_r''\varepsilon_r'' - \mu_r'\varepsilon_r')^2 + (\varepsilon_r'\mu_r'' + \varepsilon_r''\mu_r')}} \tag{13}$$

The input impedance of a wave absorber ($Z_{in}$) with single layer backed by a metallic reflector is given by the relation

$$Z_{in} = Z_0\sqrt{\frac{\mu_r}{\varepsilon_r}}\tanh(\gamma.t) \tag{14}$$

where $Z_0$ is the impedance of free space, and the reflection coefficient is given by the relation

$$\Gamma = \frac{Z_{in} - Z_0}{Z_{in} + Z_0} \tag{15}$$

and reflection loss expressed in decibel ($R$) is given as

$$R = 20.\log_{10}|\Gamma|dB \tag{16}$$

The electrical wavelength ($\lambda$) in the material can be calculated from the phase constant $\beta$ for any given frequency as

$$\lambda = 2.\pi/\beta \tag{17}$$

At the air–material interface total cancellation of reflected wave can occur because of interference between the incident and the reflected waves. The condition for this can be deduced assuming that the dielectric loss in the medium is small compared to the dielectric permittivity [21]. The equation can be expressed as

$$t_0 = \frac{c}{4.f}\frac{1}{\sqrt{\mu_r'\varepsilon_r'}}\left(1 + \frac{1}{8}\tan^2\delta_\mu\right)^{-1} \tag{18}$$

where $\delta_\mu$ is the magnetic loss tangent.

Based on the previously given equations, the propagation constant of the composites was calculated and from which the reflection loss at various frequencies was estimated. In our studies the magnetic permeability and dielectric permittivity were not measured for the same frequencies, since the measurements were carried out at even and odd resonating modes of the cavity. The real part of the permittivity of a particular sample nearly remains a constant in the entire frequency range of X band, and the average value of this permittivity was assumed to be valid for all frequencies and used in the calculations. The values of $\varepsilon_r''$, $\mu'$, and $\mu''$ were estimated for the entire range of X band in steps of 0.1 GHz by interpolating the plots with the help of a commercial computer software for extrapolation and interpolation of graphs.

For natural-rubber-based composites the refection loss with the frequency does not show any resonance and shows a steady decrease with the increase in frequency (Fig. 14). A maximum of −10.5-dB loss is registered for a frequency of 12 GHz. The thickness corresponding to the cancellation of the reflected waves by interference also decreases steadily with the frequency as depicted in Fig. 15

For neoprene-rubber-based composites the variation of reflection loss with frequency is shown in Fig. 16. It can be observed from the graphs that the frequency corresponding to the maximum reflection loss is shifting towards the lower frequency side as the concentration of nickel particles increases in the composites. This result is consistent with previous reports. The thickness for cancellation of reflected wave is calculated and the results are shown in Fig. 17. There is a steady decrease in thickness corresponding to a total annihilation of waves by interference.

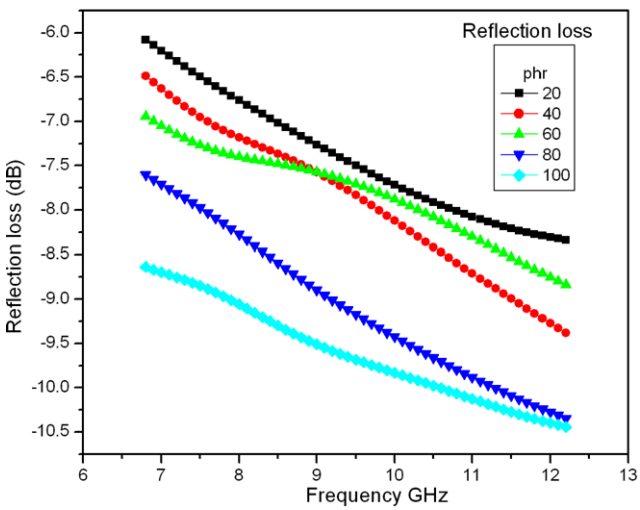


**Fig. 14** Calculated reflection loss of natural-rubber–nickel composites

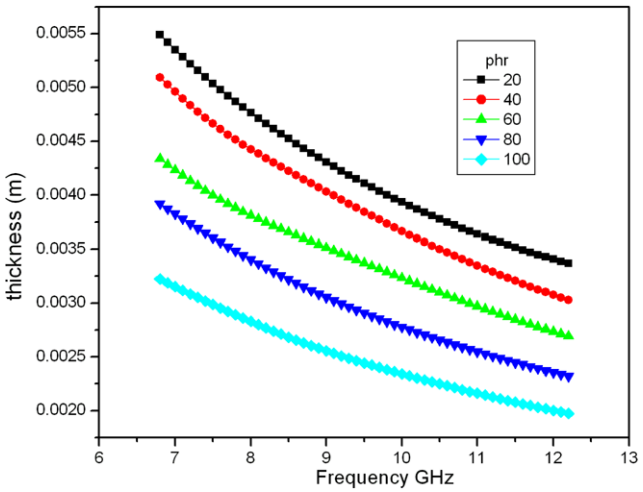


**Fig. 15** Variation in thickness of natural-rubber–nickel composites corresponding to complete annihilation of EM waves

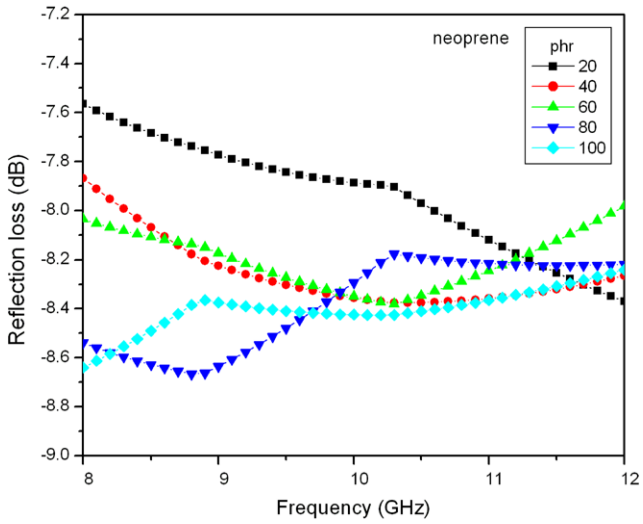


**Fig. 16** Calculated reflection loss of neoprene-rubber–nickel composites

## 4 Conclusion

The complex dielectric permittivity and magnetic permeability of natural-rubber–nickel and neoprene-rubber–nickel nanocomposites were evaluated in the X band of microwave frequencies from 7 to 12 GHz. The real part of dielectric permittivity does not change with the frequency but registers a steady increase with the increase in the concentration of loading of nickel nanoparticles. The dielectric loss shows an increase with the frequency in general and for natural-rubber-based composites there appears a shallow relaxation peak at around 8.25 GHz. In both type of composites, a dielectric loss increases with an increase in the concentration of filler and a conductance loss is attributed to this observation. Real part of permeability shows a steady decrease with

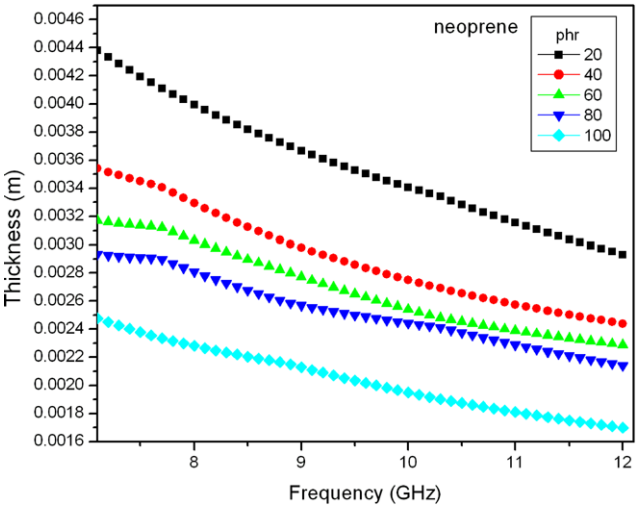


**Fig. 17** Variation in thickness of neoprene-rubber–nickel composites corresponding to complete annihilation of EM waves

an increase in frequency and the behavior is closely similar in both types of composites. The magnetic loss shows a small relaxation at 8 GHz and then decreases. Magnetic resonance of ferromagnetic nickel particles is attributed to the observed peak in magnetic loss. The input impedance and the reflection loss were calculated and for neoprene rubber a resonance is observed and is found to shift towards a higher frequency side with an increase in concentration of nickel nanoparticles.

**Acknowledgements** Authors acknowledge KSCSTE, Kerala for the financial support provided through a project. EMAJ acknowledges UGC, India for the fellowship granted under Faculty Improvement Programme.

## References

1. S. Motojimo, Y. Noda, S. Hoshiya, Y. Hishikawa, J. Appl. Phys. **94**(4), 2325–2330 (2003)
2. P.S. Neelakanta, J.C. Park, IEEE Trans. Microwave Theory Tech. **43**(6), 1381–1383 (1995)
3. Y. He, R. Gong, Y. Nie, H. He, Z. Zhao, J. Appl. Phys. **98**, 084903 (2005)
4. D. Rousselle, A. Berthault, O. Acher, J.P. Bouchaud, P.G. Zerah, J. Appl. Phys. **74**, 475 (1993)
5. S. Sugimoto, T. Maeda, D. Book, T. Kagotani, K. Inomata, M. Homma, H. Ota, Y. Houjou, R. Sato, J. Alloys Compd. **330**, 301 (2002)
6. J.R. Liu, M. Itoh, T. Horikawa, K. Machida, J. Appl. Phys. **98**, 054305 (2005)
7. B.-W. Li, Y. Shen, Z.-X. Yue, C.-W. Nan, Appl. Phys. Lett. **89**, 132504 (2006)
8. A. Bahadoor, Y. Wang, M.N. Afsar, J. Appl. Phys. **97**, 10F105 (2005)
9. J.E. Atwater, Appl. Phys. A **75**, 555–558 (2002)
10. L. Stepan, PIERS Online **4**(6), 686–690 (2008)
11. D.D.L. Chung, *Composite Materials: Science and Applications, Functional Materials for Modern Technologies* (Springer, Berlin, 2003), p. 93

12. M. Morton, *Rubber Technology*, 3rd edn. (Van Nostrand Reinhold, New York, 1995)
13. K.A. Malini, P. Kurian, M.R. Anantharaman, Mater. Lett. **57**(22–23) 3381–3386 (2003)
14. K.H. Prema, P. Kurian, P.A. Joy, M.R. Anantharaman, Polym.-Plast. Technol. Eng. **47**(2), 137–146 (2008)
15. Y. Yan, A. Sklyuyev, C. Akyel, P. Ciureanu, in Proc. Instrumentation and Measurement Technology Conference, 2007 IEEE 1–3 May 2007, pp. 1–6. doi:10.1109/IMTC.2007.379006
16. M. Lin, Y. Wang, M.N. Afsar, in 13th International Conference on Terahertz Electronics, Infrared and Millimeter Waves (2005). IRMMW-THz 2005. The Joint 30th International Conference, vol. 1, 19–23 Sept. 2005, pp. 62–63. doi:10.1109/ICIMW.2005.1572407
17. H.V. Keer, *Principles of Solid State Physics* (Wiley Eastern, New Delhi, 1998)
18. W. Gong, H. Li, Z. Zhao, J. Chen, J. Appl. Phys. **69**, 5119 (1991)
19. O. Masala, R. Seshadri, Chem. Phys. Lett. **402**(1–3), 160–164 (2005)
20. Y.B. Feng, T. Qiu, C.Y. Shen, X. Li, IEEE Trans. Magn. **42**(3), 363–368 (2006)
21. B. Zhang, Y. Feng, J. Xiong, Y. Yang, H. Lu, IEEE Trans. Magn. **42**(7), 1778–1781 (2006)